

DOI: 10.1002/cctc.201402353

Bimetallic Nickel–Rhodium Nanoparticles Supported on ZIF-8 as Highly Efficient Catalysts for Hydrogen Generation from Hydrazine in Alkaline Solution

Bingquan Xia,^[a] Nan Cao,^[a] Hongmei Dai,^[a] Jun Su,^[c] Xiaojun Wu,^[a] Wei Luo,^{*[a, b]} and Gongzhen Cheng^[a]

Highly dispersed bimetallic Ni–Rh nanoparticles with an average diameter of (1.2 ± 0.2) nm were successfully deposited on the metal–organic framework (MOF) ZIF-8 by using a simple liquid impregnation method. These catalysts were composition dependent toward the dehydrogenation of hydrazine in alkaline solution, whereas $\text{Ni}_{66}\text{Rh}_{34}@ZIF-8$ exhibited the highest catalytic activity among all the catalysts tested with a turnover frequency value of 140 h^{-1} and 100% hydrogen selectivity at 50°C . The excellent catalytic performance may be caused by the synergistic molecular-scale alloying effect of the bimetallic Ni–Rh nanoparticles on ZIF-8 and the promotion effect of ZIF-8. The development of high-performance catalysts by utilizing MOFs as a novel porous catalyst support to control the limited growth of metal nanoparticles may promote the application of hydrous hydrazine as a promising chemical hydrogen-storage material and open up new opportunities to use MOF-supported metal nanoparticles for more applications.

The search for safe and effective hydrogen-storage materials is still one of the most challenging obstacles for the development of hydrogen fuel-cell technology. Over the past decades, numerous hydrogen-storage approaches have been explored, including metal hydrides,^[1] sorbent materials,^[2] and chemical hydride systems.^[3] Among them, hydrous hydrazine ($\text{N}_2\text{H}_4 \cdot \text{H}_2\text{O}$) is considered as a promising chemical hydrogen material because of its high hydrogen content (8.0 wt%) and safe handling, the ease with which it can be recharged, and the fact that only nitrogen in addition to hydrogen are produced through a complete decomposition route, as shown in Equation (1).^[4] Moreover, hydrazine monohydrate is a liquid-phase material that has the potential to take advantage of the existing liquid-based distribution infrastructure, which makes hydra-

zine monohydrate more competitive than solid chemical hydrogen-storage materials such as sodium borohydride (NaBH_4) and ammonia borane (NH_3BH_3) derivatives. However, from the perspective of hydrogen-storage applications, the incomplete decomposition to ammonia, which is toxic to fuel-cell catalysts, by another pathway [Eq. (2)] should be avoided. Recently, a number of noble and non-noble metal-containing mono- and bimetallic nanocatalysts have been developed.^[5] How to strike a balance between cost, selectivity, efficiency, and recyclability, however, still remains a considerable challenge.



On the other hand, as a new class of hybrid functional materials and owing to their high porosity, large surface area, and chemical tenability, metal–organic frameworks (MOFs) have attracted growing attention in a variety of applications, such as gas storage,^[6] gas separation,^[7] heterogeneous catalysis,^[8] sensing,^[9] and drug delivery.^[10] Given their similarity to zeolites, loading metal nanoparticles (NPs) into the pores of MOFs is expected to control the limited growth of the metal NPs in the confined cavities and limit the migration and aggregation of the metal NPs, and thus further increase their catalytic activity and stability. Loading metal NPs inside the pores of MOFs is of current interest. Until now, a number of monometallic Pd, Pt, Ir, Au, and Ru NPs and their bimetallic alloy NPs with non-noble metals have been successively immobilized into the pores of MOFs.^[11] As far as we know, however, there is no report on MOF-supported Rh-based NPs with full characterization.^[12] Herein, we report the first MOF-supported Ni–Rh bimetallic NPs. We study the synergistic effect of metal composition in the MOFs for the catalytic dehydrogenation of hydrazine in alkaline solution. The ZIF-8 framework [$\text{Zn}(\text{MeIm})_2$, MeIm = 2-methylimidazole], one of the preventative MOFs, was used as a support because of its intersecting 3D structure, high thermal and chemical stability, and large surface area.^[13] Relative to the activity of other reported catalysts for the dehydrogenation of hydrazine, the $\text{Ni}_{66}\text{Rh}_{34}@ZIF-8$ catalyst exhibits the highest catalytic activity with a turnover frequency (TOF) value of 140 h^{-1} and 100% hydrogen selectivity at 50°C .

The bimetallic Ni–Rh NPs with different Ni–Rh compositions were successfully immobilized by ZIF-8 through a simple liquid impregnation method. Activated ZIF-8 (100 mg) was impregnated with deionized water (4 mL) containing a total of

[a] B. Xia, N. Cao, H. Dai, Dr. X. Wu, Prof. W. Luo, Prof. G. Cheng
College of Chemistry and Molecular Sciences
Wuhan University
Wuhan, Hubei 430072 (P.R. China)
E-mail: wluo@whu.edu.cn

[b] Prof. W. Luo
Suzhou Institute of Wuhan University
Suzhou, Jiangsu, 215123 (P.R. China)

[c] Dr. J. Su
Wuhan National Laboratory for Optoelectronics
Huazhong University of Science and Technology
Wuhan, Hubei, 430074 (P.R. China)

 Supporting information for this article is available on the WWW under <http://dx.doi.org/10.1002/cctc.201402353>.

0.2 mmol of nickel chloride and rhodium chloride in different molar ratios (1:9, 2:8, 4:6, 7:3, 9:1) at 298 K for 12 h. To obtain the NiRh@ZIF-8 catalysts, the as-synthesized samples were separated by centrifugation and dried, which was followed by reduction by using sodium borohydride at 273 K. The final ratio of Ni and Rh in the catalysts was determined by inductively coupled plasma atomic emission spectroscopy (ICP-AES), which was close to the initial loading (Table S1, Supporting Information). The powder X-ray diffraction (PXRD) patterns of as-synthesized ZIF-8, Ni@ZIF-8, Rh@ZIF-8, and Ni₆₆Rh₃₄@ZIF-8 revealed no loss of crystallinity, as shown in Figure S1, and this indicates that the integrity of the ZIF-8 framework was maintained during catalyst preparation. Furthermore, no clear diffraction peaks of Ni or Rh were detected, probably as a result of the low concentrations and small sizes of the NPs immobilized by ZIF-8 (see below). The N₂ adsorption–desorption isotherms of ZIF-8 and Ni₆₆Rh₃₄@ZIF-8 are shown in Figure S2a, and they further confirm the high stability of the porous structure of ZIF-8. The specific areas were 1644 and 786 m²g⁻¹ for ZIF-8 and Ni₆₆Rh₃₄@ZIF-8, respectively. A significant decrease in the amount of N₂ adsorption and a decrease in the pore volume (Figure S2b) of Ni₆₆Rh₃₄@ZIF-8 indicate that the cavities of ZIF-8 were either occupied by the well-dispersed Ni–Rh NPs or blocked by the Ni–Rh NPs. The morphology of Ni₆₆Rh₃₄@ZIF-8 was further characterized by transmission electron microscopy (TEM) and energy-dispersive X-ray spectroscopy (EDX) measurements (Figure 1). Well-dispersed Ni–Rh NPs, with an average diameter of (1.2 ± 0.2) nm, were encapsulated in the cages of ZIF-8, which may explain the high catalytic activity and durability for the dehydrogenation of hydrazine (see below). A representative high-resolution TEM image in Figure 1c shows the *d* spacing of 0.215 nm, which is between the

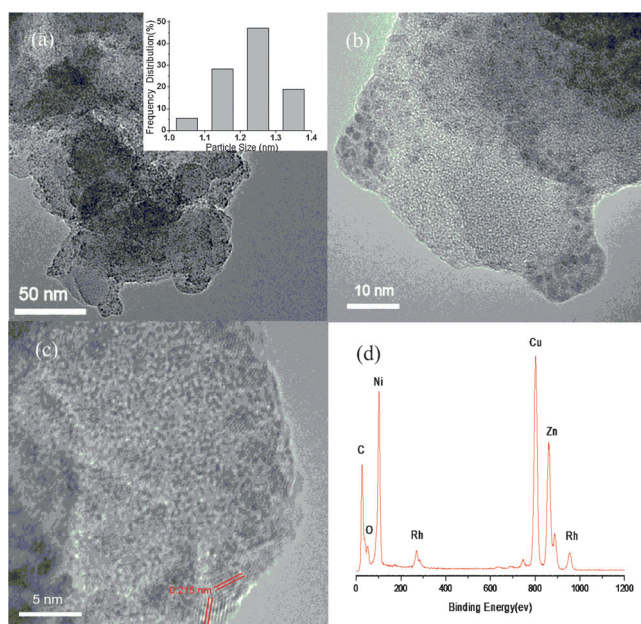


Figure 1. a–c) TEM images of Ni₆₆Rh₃₄@ZIF-8 at different magnifications. The inset in a) shows the particle-size distribution of the Ni₆₆Rh₃₄ NPs. d) EDX of Ni₆₆Rh₃₄@ZIF-8.

{111} lattice spacing of face-centered cubic (fcc) Ni (0.203 nm) and fcc Rh (0.219 nm); this suggests that Ni–Rh is formed as an alloy structure. The EDX spectra (Figure 1d) further confirmed the presence of Ni–Rh. In addition, X-ray photoelectron spectroscopy (XPS) measurements were performed to understand the states of Rh and Ni that coexist in the catalyst, for which characteristic signals of both metals were detected (Figure S3), and this demonstrated the composition of Ni⁰ and Rh⁰ in the NiRh@ZIF-8 catalyst. The observed Ni 2p_{3/2} and Ni 2p_{1/2} binding energies at 856.5 and 874.6 eV, respectively, correspond to Ni⁰, and the Rh 3d_{5/2} and Rh 3d_{3/2} binding energies at 310.3 and 314.8 eV, respectively, correspond to Rh⁰.^[14]

The catalytic dehydrogenation of hydrazine was performed over all the samples at 50 °C in the presence of NaOH (0.5 M), as shown in Figure 2. The activities of the catalysts were

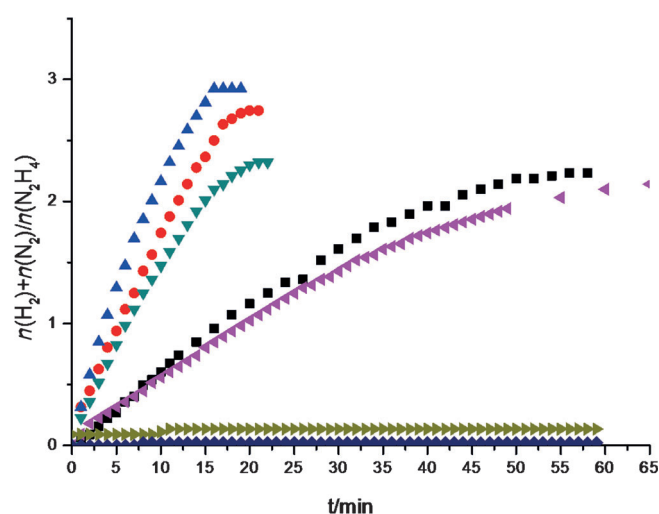


Figure 2. Time course plots for the decomposition of hydrazine in aqueous NaOH solution (0.5 M) catalyzed by a) Ni₉Rh₉@ZIF-8 (■), b) Ni₈₂Rh₁₈@ZIF-8 (●), c) Ni₆₆Rh₃₄@ZIF-8 (▲), d) Ni₃₅Rh₆₅@ZIF-8 (▼), e) Ni₁₄Rh₈₆@ZIF-8 (◆), f) Rh@ZIF-8 (►), and g) Ni@ZIF-8 (◄). Catalyst = 0.100 g, N₂H₄·H₂O = 0.1 mL.

strongly dependent on the Ni–Rh compositions; whereas Ni@ZIF-8 and Rh@ZIF-8 were catalytically inactive, Ni₃₅Rh₆₅@ZIF-8 presented poor catalytic activity (only about 2 equiv. gas was released over 1 h) and low hydrogen selectivity (70%). Among all the bimetallic NiRh@ZIF-8 samples investigated, Ni₆₆Rh₃₄@ZIF-8 exhibited the highest catalytic activity, with a TOF value of 140 h⁻¹ at 50 °C, which is the highest value among all the reported catalysts (Table 1); this highlights the synergistic effect of molecular-scale Ni–Rh alloying compositions in ZIF-8 for their catalytic activity. The H₂ selectivity and completeness of hydrazine decomposition over Ni₆₆Rh₃₄@ZIF-8 were further confirmed by mass spectrometry (Figure S4), which indicated 100% H₂ selectivity. Furthermore, as a control experiment, the same amount of Ni₆₆Rh₃₄ NPs and ZIF-8 were synthesized and applied to the dehydrogenation of an alkaline solution of hydrazine. As shown in Figure S5, only 2.36 equivalents of gas with 76% H₂ selectivity was released over 60 min for the Ni–Rh NPs, and almost no reactivity for ZIF-8 was observed in the dehydrogenation of an alkaline solution of hydra-

Table 1. Comparison of the activities of the different catalysts in the generation of hydrogen through the decomposition of $\text{H}_2\text{NNH}_2\cdot\text{H}_2\text{O}$ in aqueous solution.

Catalyst	T [K]	TOF [h^{-1}]	E_a [kJ mol^{-1}]	Ref.
NiRh_4	298	9.6	–	[15]
$\text{Ni}_{66}\text{Rh}_{10}$	323	4.5	–	[5f]
$\text{NiRh}_4/\text{graphene}$	298	20	–	[5g]
$\text{Ni}_{66}\text{Rh}_{34}@\text{ZIF-8}$	323	140	58.1	this work
$\text{Ni}_{10.6}\text{Pd}_{0.4}$	323	6	–	[4f]
$\text{Ni}_{10.99}\text{Pt}_{0.01}$	323	6	49.95	[16]
$\text{NiPt}_{0.057}/\text{Al}_2\text{O}_3$	303	16.5	49.3	[4b]
$\text{Ni}_{80}\text{Pt}_{20}@\text{ZIF-8}$	323	90	–	[11g]
$\text{Ni}_{10.9}\text{Pt}_{0.1}/\text{Ce}_2\text{O}_3$	298	28.1	42.3	[4a]
$\text{Ni}_{10.95}\text{Ir}_{0.05}$	298	4.5	–	[5b]
$\text{Ni}/\text{Al}_2\text{O}_3$	303	2.2	34	[4b]

zine at 50°C ; this is indicative of the synergetic effect of the Ni–Rh NPs and the framework of ZIF-8.

To obtain the activation energy (E_a) of the dehydrogenation of an alkaline solution of hydrazine catalyzed by $\text{Ni}_{66}\text{Rh}_{34}@\text{ZIF-8}$, reactions were performed at temperatures ranging from 50 to 80°C (Figure S6), and the value of E_a was determined to be $58.01 \text{ kJ mol}^{-1}$, which is close to the reported value (Table 1).

Furthermore, we tested the stability of the $\text{Ni}_{66}\text{Rh}_{34}@\text{ZIF-8}$ catalyst in the dehydrogenation of an alkaline solution of hydrazine at 50°C (Figure S7). The results showed that there was no significant decrease in catalytic activity and no change in the hydrogen selectivity even after the fifth run.

In summary, well-dispersed Ni–Rh NPs have been immobilized on the framework of ZIF-8 and exhibit high catalytic activity and durability toward hydrogen generation from aqueous hydrazine solution. Furthermore, it is expected that this simple liquid impregnation synthetic method could be extended to other MOF-supported bimetallic or polymetallic metal NPs for further application.

Experimental Section

Chemicals and materials

All chemicals were commercial and were used without further purification. Zinc nitrate hexahydrate [$\text{Zn}(\text{NO}_3)_2\cdot 6\text{H}_2\text{O}$, Sinopharm Chemical Reagent Co., Ltd., 99%], nickel chloride hexahydrate ($\text{NiCl}_2\cdot 6\text{H}_2\text{O}$, Sinopharm Chemical Reagent Co., Ltd., $\geq 99\%$), rhodium chloride trihydrate ($\text{RhCl}_3\cdot 3\text{H}_2\text{O}$, Adamas Reagent Co., Ltd., 99%), hydrazine monohydrate ($\text{H}_2\text{N}_2\cdot\text{H}_2\text{O}$, TCI Shanghai Co., Ltd., $> 98\%$), aqueous hydrofluoric acid (HF, Sinopharm Chemical Reagent Co., Ltd., 40%), sodium borohydride (NaBH_4 , Sinopharm Chemical Reagent Co., Ltd., 96%), and ethanol ($\text{C}_2\text{H}_5\text{OH}$, Sinopharm Chemical Reagent Co., Ltd., $> 99.8\%$) were used as received. We used ordinary distilled water as the reaction solvent.

Synthesis of ZIF-8

ZIF-8 was synthesized by using a reported procedure.^[13b] $\text{Zn}(\text{NO}_3)_2\cdot 6\text{H}_2\text{O}$ (350 mg) and 2-methylimidazole (200 mg) were placed in a 20 mL screw-top vial and dissolved in DMF (15 mL). Three drops of HNO_3 were added to the mixture by using a Pasteur

pipet, and complete dissolution was achieved by sonication. The vial was capped and placed in an oven at 120°C for 24 h. ZIF-8 crystals were collected and washed with DMF. The crystals were stored in DMF until needed for experiments.

Preparation of the catalyst

Prior to metal loading, as-prepared ZIF-8 was pretreated as follows: ZIF-8 was immersed in methanol under ambient conditions for 48 h and then evacuated at room temperature for over 10 h and at 573 K for 2 h to obtain optimally evacuated sample. The NiRh@ZIF-8 catalysts were synthesized by a simple liquid impregnation method. A typical synthesis procedure for the catalyst is described: Activated ZIF-8 (100 mg) was mixed with $\text{RhCl}_3\cdot 3\text{H}_2\text{O}$ (0.02 mmol) and $\text{NiCl}_2\cdot 6\text{H}_2\text{O}$ (0.18 mmol) in deionized water (10 mL). The solution was continuously stirred for 12 h at 25°C to impregnate the metal salts. After impregnation, the suspension was concentrated under vacuum. The resulting mixture was then reduced by using sodium borohydride (NaBH_4 , 78.6 mg) with vigorous stirring at 273 K to yield $\text{Ni}_{14}\text{Rh}_{86}@\text{ZIF-8}$. The preparations of $\text{Ni}_{35}\text{Rh}_{65}@\text{ZIF-8}$, $\text{Ni}_{66}\text{Rh}_{34}@\text{ZIF-8}$, $\text{Ni}_{82}\text{Rh}_{18}@\text{ZIF-8}$, $\text{Ni}_{91}\text{Rh}_9@\text{ZIF-8}$, $\text{Rh}@\text{ZIF-8}$, and $\text{Ni}@\text{ZIF-8}$ followed an analogous process.

Hydrous hydrazine decomposition test

In a typical experiment, $\text{Ni}_{66}\text{Rh}_{34}@\text{ZIF-8}$ (100 mg) and NaOH (80 mg) were dissolved in water (4 mL) in a two-necked round-bottomed flask with vigorous stirring. One neck of the flask was connected to a gas burette to monitor the volume of gas evolution, and the other neck was used to introduce hydrazine monohydrate (0.1 mL, 1.96 mmol). A water bath was used to control the temperature of the solution at 323 K. The gas released during the reaction was passed through 1.0 M HCl before it was measured volumetrically. The selectivity towards H_2 generation (X) can be calculated by using Equation (3):

$$X = \frac{(3\lambda - 1)}{8} \quad (3)$$

$$\lambda = \frac{n(\text{H}_2 + \text{N}_2)}{n(\text{H}_2\text{NNH}_2)}$$

To obtain the activation energy (E_a), the catalytic reaction temperature was varied from 323 to 353 K (catalyst = 100 mg; $\text{N}_2\text{H}_4\cdot\text{H}_2\text{O}$ = 0.1 mL).

Recycle stability tests

For the recycle stability test, the catalytic reactions were repeated five times by adding another equivalent of hydrous hydrazine (2 mmol) to the mixture after the previous cycle.

Characterization

The morphologies and sizes of the samples were observed by using a Tecnai G20 U-Twin transmission electron microscope equipped with an energy-dispersive X-ray detector at an acceleration voltage of 200 kV. Powder X-ray diffraction patterns were measured by using a Bruker D8-Advance X-ray diffractometer by using a CuK_α radiation source ($\lambda = 0.154178 \text{ nm}$) with a velocity of 1° min^{-1} . X-ray photoelectron spectroscopy measurements were performed with a Kratos XSAM 800 spectrophotometer. The surface area measurements were performed with N_2 adsorption-de-

sorption isotherm at liquid-nitrogen temperature (77 K) after dehydration under vacuum at 120 °C for 12 h by using a Quantachrome NOVA 4200e. Inductively coupled plasma atomic emission spectroscopy was performed with an IRIS Intrepid II XSP (Thermo Fisher Scientific, USA). Mass spectra of the generated gases were collected by using a Ametek Dycor mass spectrometer under an argon atmosphere.

Acknowledgements

This work was financially supported by the National Natural Science Foundation of China (21201134), the Natural Science Foundation of Jiangsu Province (BK20130370), the Natural Science Foundation of Hubei Province (2013CFB288), the Ministry of Science and Technology of China (2011YQ12003504), and the Large-Scale Instrument and Equipment Sharing Foundation of Wuhan University.

Keywords: dehydrogenation · hydrogen storage · metal-organic frameworks · nanoparticles · nickel

- [1] F. Schüth, B. Bogdanovic, M. Felderhoff, *Chem. Commun.* **2004**, 2249–2258.
- [2] a) S.-L. Li, Q. Xu, *Energy Environ. Sci.* **2013**, *6*, 1656–1683; b) Q. Xiang, J. Yu, M. Jaroniec, *Chem. Soc. Rev.* **2012**, *41*, 782–796.
- [3] W. Luo, P. G. Campbell, L. N. Zakharov, S.-Y. Liu, *J. Am. Chem. Soc.* **2011**, *133*, 19326–19329.
- [4] a) H.-L. Wang, J.-M. Yan, Z.-L. Wang, S.-I. O, Q. Jiang, *J. Mater. Chem. A* **2013**, *1*, 14957–14962; b) L. He, Y. Huang, A. Wang, Y. Liu, X. Liu, X. Chen, J. J. Delgado, X. Wang, T. Zhang, *J. Catal.* **2013**, *298*, 1–9; c) K. Aranishi, A. K. Singh, Q. Xu, *ChemCatChem* **2013**, *5*, 2248–2252; d) J. Zhang, Q. Kang, Z. Yang, H. Dai, D. Zhuang, P. Wang, *J. Mater. Chem. A* **2013**, *1*, 11623–11628; e) S. K. Singh, Q. Xu, *Catal. Sci. Technol.* **2013**, *3*, 1889–1900; f) S. K. Singh, Y. Iizuka, Q. Xu, *Int. J. Hydrogen Energy* **2011**, *36*, 11794–11801.
- [5] a) S. K. Singh, A. K. Singh, K. Aranishi, Q. Xu, *J. Am. Chem. Soc.* **2011**, *133*, 19638–19641; b) S. K. Singh, Q. Xu, *Chem. Commun.* **2010**, *46*, 6545–6547; c) S. K. Singh, Q. Xu, *Inorg. Chem.* **2010**, *49*, 6148–6152; d) S. K. Singh, X.-B. Zhang, Q. Xu, *J. Am. Chem. Soc.* **2009**, *131*, 9894–9895; e) D. G. Tong, W. Chu, P. Wu, G. F. Gu, L. Zhang, *J. Mater. Chem. A* **2013**, *1*, 358–366; f) A. K. Singh, M. Yadav, K. Aranishi, Q. Xu, *Int. J. Hydrogen Energy* **2012**, *37*, 18915–18919; g) J. Wang, X.-B. Zhang, Z.-L. Wang, L.-M. Wang, Y. Zhang, *Energy Environ. Sci.* **2012**, *5*, 6885–6888.
- [6] N. L. Rosi, J. Eckert, M. Eddaoudi, D. T. Vodak, J. Kim, M. O’Keeffe, O. M. Yaghi, *Science* **2003**, *300*, 1127–1130.
- [7] J.-R. Li, R. J. Kuppler, H.-C. Zhou, *Chem. Soc. Rev.* **2009**, *38*, 1477–1504.
- [8] J. Y. Lee, O. K. Farha, J. Roberts, K. A. Scheidt, S. B. T. Nguyen, J. T. Hupp, *Chem. Soc. Rev.* **2009**, *38*, 1450–1459.
- [9] L. E. Kreno, K. Leong, O. K. Farha, M. Allendorf, R. P. Van Duyne, J. T. Hupp, *Chem. Rev.* **2012**, *112*, 1105–1125.
- [10] J. Della Rocca, D. Liu, W. Lin, *Acc. Chem. Res.* **2011**, *44*, 957–968.
- [11] a) H. Dai, J. Su, K. Hu, W. Luo, G. Cheng, *Int. J. Hydrogen Energy* **2014**, *39*, 4947–4953; b) A. Aijaz, A. Karkamkar, Y. J. Choi, N. Tsumori, E. Ronnebro, T. Autrey, H. Shioyama, Q. Xu, *J. Am. Chem. Soc.* **2012**, *134*, 13926–13929; c) M. Zahmakiran, *Dalton Trans.* **2012**, *41*, 12690–12696; d) D. Esken, S. Turner, O. I. Lebedev, G. Van Tendeloo, R. A. Fischer, *Chem. Mater.* **2010**, *22*, 6393–6401; e) X. Gu, Z.-H. Lu, H.-L. Jiang, T. Akita, Q. Xu, *J. Am. Chem. Soc.* **2011**, *133*, 11822–11825; f) J. Long, H. Liu, S. Wu, S. Liao, Y. Li, *ACS Catal.* **2013**, *3*, 647–654; g) A. K. Singh, Q. Xu, *ChemCatChem* **2013**, *5*, 3000–3004.
- [12] There is one example regarding Rh@MOF-5, but only characterized by PXRD and FITR, see T. Van Vu, H. Kosslick, A. Schulz, J. Harloff, E. Paetzold, H. Lund, U. Kragl, M. Schneider, G. Fulda, *Microporous Mesoporous Mater.* **2012**, *154*, 100–106.
- [13] a) K. S. Park, Z. Ni, A. P. Côté, J. Y. Choi, R. Huang, F. J. Uribe-Romo, H. K. Chae, M. O’Keeffe, O. M. Yaghi, *Proc. Natl. Acad. Sci. USA* **2006**, *103*, 10186–10191; b) O. Karagiari, M. B. Lalonde, W. Bury, A. A. Sarjeant, O. K. Farha, J. T. Hupp, *J. Am. Chem. Soc.* **2012**, *134*, 18790–18796.
- [14] Y. L. Qin, J. Wang, F. Z. Meng, L. M. Wang, X. B. Zhang, *Chem. Commun.* **2013**, *49*, 10028–10030.
- [15] S. K. Singh, Q. Xu, *J. Am. Chem. Soc.* **2009**, *131*, 18032–18033.
- [16] S. K. Singh, Z. H. Lu, Q. Xu, *Eur. J. Inorg. Chem.* **2011**, 2232–2237.

Received: May 19, 2014

Revised: June 23, 2014

Published online on August 19, 2014